RAA 2021 Vol. **21** No. **10**, 252(11pp) doi:10.1088/1674-4527/21/10/252

http://www.raa-journal.org *http://iopscience.iop.org/raa*

***R**esearch in*
***A**stronomy and*
***A**strophysics*

Effects of displacement current on wave dispersion relation and polarization properties in auroral plasmas

Liang Xiang[1,2], Bing Ma[3,4], Qiu-Huan Li[1⋆], Ling Chen[3], Hong-Wei Yu[2] and De-Jin Wu[3]

[1] Institute of Space Physics, Luoyang Normal University, Luoyang 471934, China; *liqiuhuan@csust.edu.cn*
[2] Department of Physics and Synergetic Innovation Center for Quantum Effects and Applications, School of Physics and Electronics, Hunan Normal University, Changsha 410081, China
[3] Key Laboratory of Planetary Sciences, Purple Mountain Observatory, Chinese Academy of Sciences, Nanjing 210034, China
[4] University of Science and Technology of China, Hefei 230026, China

Received 2021 January 19; accepted 2021 June 26

Abstract In-situ observations from the FREJA magnetospheric research satellite and the Fast Auroral SnapshoT satellite have shown that plasma waves are frequently observed in the auroral plasma, which are believed to be fundamentally important in wave energy dissipation and particle energization. However, the effects of a displacement current on these waves have not been examined. Based on the two-fluid theory, we investigate the dispersion relation and polarization properties of fast, Alfvén, and slow modes in the presence of a displacement current, and the effects of the displacement current on these waves are also considered. The results show that the wave frequency, polarization, magnetic helicity and other properties for the fast and Alfvén modes are highly sensitive to the normalized Alfvén velocity v_A/c, plasma beta β, and propagation angle θ, while for the slow mode the dependence is minor. In particular, for both fast and Alfvén modes, the magnetic helicity is obviously different with and without the displacement current, especially for the Alfvén mode with the helicity reversals from right-handed to left-handed when v_A/c increases from 0 to 0.3. The charge-neutral condition of both fast and Alfvén modes with frequencies larger than the proton cyclotron frequency is invalid in the presence of the displacement current. Moreover, the presence of the displacement current leads to relatively large magnetic compressibility for the Alfvén mode and relatively large electron compressibility for the fast mode. These results can be useful for a comprehensive understanding of the wave properties and the physics of particle energization phenomena in auroral plasmas.

Key words: waves — magnetohydrodynamics (MHD) — planets and satellites: aurorae

1 INTRODUCTION

The auroral zone is one of the most fascinating regions in the magnetosphere and there exist a variety of plasma physical processes, including the formation of the electric field, particle acceleration, microphysics of plasma instabilities, and radio emissions (Kaufmann 1984; Bespalov et al. 2006; Wu & Chen 2020). In-situ observations from Earth auroral satellites, the FREJA magnetospheric research satellite (FREJA) and the Fast Auroral SnapshoT (FAST) satellite, have shown that a variety of plasma waves exist ubiquitously in auroral plasmas with a low-beta regime of $\beta < m_e/m_i$, such as magnetohydrodynamics (MHD) Alfvén wave, kinetic Alfvén wave, ion-acoustic wave, ion cyclotron wave, fast wave, and whistler wave (Hofstee & Forsyth 1969; Cattell et al. 1998; Lund et al. 1998; Chaston et al. 2004, 2005), where β is the ratio of plasma pressure to magnetic pressure. Moreover, the spacecraft measurements have shown that plasma waves carry the Poynting flux strong enough to induce efficient plasma heating and particle acceleration in the auroral plasma through wave-particle interactions (Lysak & Song 2003; Seyler & Liu 2007; Swift 2007).

In-situ auroral plasma observations, e.g., from FREJA and FAST, have shown that the auroral plasma parameters have a wide regime with the density varying from

⋆ Corresponding author

$10^6\,\mathrm{cm}^{-3}$ to less than $10^{-2}\,\mathrm{cm}^{-3}$, the temperature from 0.1 eV to 10 keV, and the magnetic field from 0.5 G to 50 nT in the altitudes from 10^2 km to about 10^5 km (Mozer et al. 1980; Kletzing & Torbert 1994; Kletzing et al. 1998; Wu & Chao 2004). These plasma parameters determine the local Alfvén velocity v_{A}, which has a higher value in the acceleration region between $0.7\,R_{\mathrm{E}}$ and $1.88\,R_{\mathrm{E}}$ and reaches its maximal value of $v_{\mathrm{A}}/c = 0.2$ near $1\,R_{\mathrm{E}}$ (Stasiewicz et al. 2000; Wu & Chao 2003), where R_{E} and c represent the Earth's radius and light velocity, respectively. Therefore, the effects associating with the normalized Alfvén velocity of v_{A}/c cannot be neglected in the studies of plasma waves in auroral plasmas.

In homogeneous magnetized two-fluid plasmas, there are three well-known electromagnetic modes with frequencies less than the electron cyclotron frequency: the fast, Alfvén, and slow modes (Cramer 2001; Swanson 2003). The dispersion relation and polarizations have been extensively studied using different formulations for a number of plasma waves, such as MHD Alfvén wave, slow wave, fast wave, kinetic Alfvén wave, kinetic slow wave, ion-cyclotron wave, fast wave and whistler wave (Hollweg 1999; Gary & Borovsky 2004; Lu & Li 2007; Gary & Smith 2009; Bellan 2012; Sahraoui et al. 2012; Boldyrev et al. 2013; Xiang et al. 2019). Based on the two-fluid theory, Zhao (2015) obtained the general dispersion relation and polarizations for low-frequency waves with frequencies less than the electron cyclotron frequency. However, their discussion is just in the limit of $v_{\mathrm{A}}/c \ll 1$, that is, the displacement current in the Ampere's law has been ignored (Lysak & Lotko 1996; Zhao et al. 2014). A comprehensive investigation of the wave dispersion relation and polarization properties in the presence of a displacement current is still lacking in auroral plasmas. In this paper, based on the complete set of two-fluid and Maxwell' equations, we study the effects of a displacement current on the wave dispersion relation and polarization properties. Our results show that the wave frequency, polarization, and other properties are sensitive to the normalized Alfvén velocity v_{A}/c and the plasma beta β, as well as the propagation angle θ. The polarization and helicity properties have potential importance in understanding the physics of wave-particle interaction in auroral plasmas.

The rest of the paper is organized as follows. First, based on the two-fluid theory, the basic physical model and the wave equation are derived in Section 2. Then, the effects of the displacement current on the wave dispersion relation and polarization properties at different propagation angles θ, different v_{A}/c regimes, and different β regimes are investigated in Section 3. Finally, Section 4 is devoted to our discussion and conclusion.

2 PLASMA MODEL AND WAVE EQUATION

In an electron-proton plasma magnetized by an ambient magnetic field along the z direction (i.e., $\boldsymbol{B_0} = B_0\boldsymbol{e_z}$), the complete set of two-fluid equation and Maxwell's equations can be written as follows:

$$m_\alpha n_0 \frac{\partial \boldsymbol{\delta v_\alpha}}{\partial t} = n_0 q_\alpha \left(\boldsymbol{\delta E} + \boldsymbol{\delta v_\alpha} \times \boldsymbol{B_0}\right) - \nabla \delta P_\alpha, \quad (1)$$

$$\frac{\partial \delta n_\alpha}{\partial t} = -\nabla \cdot \left(n_0 \boldsymbol{\delta v_\alpha}\right), \quad (2)$$

$$\delta P_\alpha = \kappa \gamma_\alpha T_\alpha \delta n_\alpha, \quad (3)$$

$$\nabla \times \boldsymbol{\delta B} = \mu_0 \boldsymbol{\delta J} + \varepsilon_0 \mu_0 \frac{\partial \boldsymbol{\delta E}}{\partial t}, \quad (4)$$

$$\nabla \times \boldsymbol{\delta E} = -\frac{\partial \boldsymbol{\delta B}}{\partial t}, \quad (5)$$

$$\nabla \cdot \boldsymbol{\delta E} = \frac{1}{\varepsilon_0} \sum_\alpha q_\alpha \delta n_\alpha, \quad (6)$$

where the subscript $\alpha = i$, e denote protons and electrons, respectively, δn_α, $\boldsymbol{\delta v_\alpha}$, $\boldsymbol{\delta E}$, $\boldsymbol{\delta B}$, δP_α, and $\boldsymbol{\delta J}$ represent the perturbed number density, velocity, electric field, magnetic field, thermal pressure, and current density, respectively. q_α, n_0, and T_α are the charge, ambient number density, and temperature, respectively. κ, γ_α, ε_0, and μ_0 are the Boltzmann constant, polyindex, permittivity, and permeability, and θ is the propagation angle between the wave vector $\boldsymbol{k}$ and the ambient magnetic field $\boldsymbol{B_0}$. We consider a plane wave form of $\delta f = \delta f_{\mathrm{k}} \exp\left(-i\omega t + i\boldsymbol{k} \cdot \boldsymbol{r}\right)$, where ω is the wave frequency, and $\boldsymbol{k} = k_\perp \boldsymbol{e_x} + k_z \boldsymbol{e_z}$ is the wave vector.

From Equations (1), (3) and (6), the current density $\boldsymbol{\delta J} = n_0 e \left(\boldsymbol{\delta v_{\mathrm{i}}} - \boldsymbol{\delta v_{\mathrm{e}}}\right)$ can be given by

$$\begin{aligned}
&\Lambda_0\Lambda_2\delta \mathrm{J}_x = \\
&- i\frac{n_0 e\omega}{B_0\omega_{\mathrm{ci}}}\left(\Lambda_2 + Q\Lambda_0 + Q\Lambda_0\frac{\varepsilon_0 B_0 \kappa T_{\mathrm{t}}}{n_0 e m_{\mathrm{i}}\omega_{\mathrm{ci}}}\tilde{T}_{\mathrm{e}} k_\perp^2\right)\delta E_{\mathrm{x}} \\
&+ \frac{n_0 e}{B_0}\left(\Lambda_2 - \Lambda_0\right)\delta E_{\mathrm{y}} - iQ\Lambda_0\frac{\omega\varepsilon_0\kappa T_{\mathrm{t}}}{m_{\mathrm{i}}\omega_{\mathrm{ci}}^2}\tilde{T}_{\mathrm{e}} k_\perp k_{\mathrm{z}}\delta E_{\mathrm{z}} \\
&- \frac{\omega n_0 e\kappa T_{\mathrm{t}}}{m_{\mathrm{i}}\omega_{\mathrm{ci}}^2}\left(\Lambda_2\tilde{T}_{\mathrm{i}} - Q\Lambda_0\tilde{T}_{\mathrm{e}}\right)k_\perp\frac{\delta n_{\mathrm{i}}}{n_0},
\end{aligned} \quad (7)$$

$$\begin{aligned}
\Lambda_0\Lambda_2\delta \mathrm{J}_y = &- \frac{n_0 e}{B_0}\left(\Lambda_2 - \Lambda_0 - \Lambda_0\frac{\varepsilon_0 B_0\kappa T_{\mathrm{t}}}{n_0 e m_{\mathrm{i}}\omega_{\mathrm{ci}}}\tilde{T}_{\mathrm{e}} k_\perp^2\right)\delta E_{\mathrm{x}} \\
&- i\frac{n_0 e\omega}{B_0\omega_{\mathrm{ci}}}\left(\Lambda_2 + Q\Lambda_0\right)\delta E_{\mathrm{y}} + \Lambda_0\frac{\varepsilon_0\kappa T_{\mathrm{t}}}{m_{\mathrm{i}}\omega_{\mathrm{ci}}}\tilde{T}_{\mathrm{e}} k_\perp k_{\mathrm{z}}\delta E_{\mathrm{z}} \\
&+ i\frac{n_0 e\kappa T_{\mathrm{t}}}{m_{\mathrm{i}}\omega_{\mathrm{ci}}}\left(\Lambda_2\tilde{T}_{\mathrm{i}} + \Lambda_0\tilde{T}_{\mathrm{e}}\right)k_\perp\frac{\delta n_{\mathrm{i}}}{n_0},
\end{aligned} \quad (8)$$

$$\begin{aligned}\delta \mathrm{J}_z = & i\frac{\varepsilon_0\kappa T_t \tilde{T}_e}{\omega m_e}k_\perp k_z \delta E_x \\ & + i\frac{e^2 n_0}{m_e\omega}\left(1+Q+\frac{\varepsilon_0\kappa T_t}{e^2 n_0}\tilde{T}_e k_z^2\right)\delta E_z \\ & + \frac{e n_0 \kappa T_t}{\omega m_e}\left(Q\tilde{T}_i - \tilde{T}_e\right)k_z \frac{\delta n_i}{n_0},\end{aligned} \tag{9}$$

where $Q = m_\mathrm{e}/m_\mathrm{i}$, $\Lambda_0 = 1-\omega^2/\omega_\mathrm{ci}^2$, $\Lambda_2 = 1-Q^2\omega^2/\omega_\mathrm{ci}^2$, $T_\mathrm{t} = \gamma_\mathrm{i} T_\mathrm{i} + \gamma_\mathrm{e} T_\mathrm{e}$, $\tilde{T}_\mathrm{i} = \gamma_\mathrm{i} T_\mathrm{i}/T_\mathrm{t}$, and $\tilde{T}_\mathrm{e} = \gamma_\mathrm{e} T_\mathrm{e}/T_\mathrm{t}$. Making use of Equations (4) and (5), we get the relation between the current density $\boldsymbol{\delta J}$ and the electric field $\boldsymbol{\delta E}$

$$\boldsymbol{\delta J} = i\frac{1}{\omega\mu_0}\left(-k^2\boldsymbol{\delta E} + \boldsymbol{kk}\cdot\boldsymbol{\delta E} + \varepsilon_0\mu_0\omega^2\boldsymbol{\delta E}\right). \tag{10}$$

Combining Equations (7) to (10), three components of the electric field can be expressed in terms of the proton number density

$$\begin{aligned} M\delta E_\mathrm{x} &= i\sin\theta B_0 v_\mathrm{T}\sqrt{\beta}k\lambda_\mathrm{i} M_\mathrm{x}\frac{\delta n_\mathrm{i}}{n_0}, \\ M\delta E_\mathrm{y} &= \sin\theta B_0 v_\mathrm{T}\sqrt{\beta}k\lambda_\mathrm{i} M_\mathrm{y}\frac{\delta n_\mathrm{i}}{n_0}, \\ M\delta E_\mathrm{z} &= i\cos\theta B_0 v_\mathrm{T}\sqrt{\beta}k\lambda_\mathrm{i} M_\mathrm{z}\frac{\delta n_\mathrm{i}}{n_0}, \end{aligned} \tag{11}$$

where the parameters M, M_x, M_y, and M_z are presented in Appendix A. Here $\lambda_\mathrm{i} = c/\omega_\mathrm{pi}$ is the proton inertial length, $\beta = v_\mathrm{T}^2/v_\mathrm{A}^2$ is the plasma beta, ω_pi is the oscillation frequency of protons, $v_\mathrm{T} = \sqrt{\kappa T_\mathrm{t}/m_\mathrm{i}}$ is the thermal velocity, and $v_\mathrm{A} = B_0/\sqrt{\mu_0 n_0 m_\mathrm{i}}$ is the Alfvén velocity.

By use of Equations (1) and (2), the number density of protons is

$$\begin{aligned} &\left[\left(\Lambda_0 + \rho_\mathrm{i}^2 k_\perp^2\right)\omega^2 - \Lambda_0 v_\mathrm{Ti}^2 k_\mathrm{z}^2\right]\frac{\delta n_\mathrm{i}}{n_0} = \\ & -i\frac{\omega^2 k_\perp}{B_0\omega_\mathrm{ci}}\delta E_\mathrm{x} + \frac{\omega k_\perp}{B_0}\delta E_\mathrm{y} + ik_\mathrm{z}\frac{e}{m_\mathrm{i}}\Lambda_0\delta E_\mathrm{z}, \end{aligned} \tag{12}$$

where $\rho_\mathrm{i} = v_\mathrm{Ti}/\omega_\mathrm{ci}$ means the proton gyroradius, and $v_\mathrm{Ti} = \sqrt{\kappa\gamma_\mathrm{i} T_\mathrm{i}/m_\mathrm{i}}$ denotes the thermal velocity of protons. Substituting Equations (11) into (12), the general dispersion relation can be derived as

$$\begin{aligned} &\left[\left(1-\frac{\omega^2}{\omega_\mathrm{ci}^2}+\sin^2\theta\tilde{T}_\mathrm{i}\beta k^2\lambda_\mathrm{i}^2\right)\frac{\omega^2}{\omega_\mathrm{ci}^2} - \cos^2\theta\tilde{T}_\mathrm{i}\beta\left(1-\frac{\omega^2}{\omega_\mathrm{ci}^2}\right)k^2\lambda_\mathrm{i}^2\right]M \\ & -\sin^2\theta\frac{\omega^2}{\omega_\mathrm{ci}^2}\beta k^2\lambda_\mathrm{i}^2 M_\mathrm{x} - \sin^2\theta\frac{\omega}{\omega_\mathrm{ci}}\beta k^2\lambda_\mathrm{i}^2 M_\mathrm{y} \\ & +\cos^2\theta\beta k^2\lambda_\mathrm{i}^2\left(1-\frac{\omega^2}{\omega_\mathrm{ci}^2}\right)M_\mathrm{z} = 0. \end{aligned} \tag{13}$$

The above wave equation represents a general dispersion equation for all plasma waves in the presence of a displacement current in the two-fluid plasma, which gives six wave modes (as shown in Fig. 1(a)-(c)), including the slow mode, Alfvén mode, fast mode, Langmuir mode, ordinary (O) mode, and extraordinary (X) mode. It should be noted that for the parallel propagation ($\theta = 0$), the O mode and X mode correspond to the left-handed polarization and right-handed polarization, respectively, and therefore they are often called the L-O mode and R-X mode (Andre 1985). If we set $k\lambda_\mathrm{i} \to 0$, Equation (13) gives two resonance frequencies: the proton cyclotron resonance $\omega = \omega_\mathrm{ci}\cos\theta$ and the electron cyclotron resonance $\omega = \omega_\mathrm{ce}\cos\theta$. From Equation (13), it is clear that the dispersion relation obtained by Zhao (2015) can be recovered by setting $v_\mathrm{A}/c = 0$, which describes a general dispersion relation for low-frequency waves in the absent of the displacement current.

Based on Equation (11), the polarization $E_\mathrm{y}/iE_\mathrm{x}$ and the magnetic helicity σ (Gary 1986) can be obtained as

$$\frac{E_y}{iE_x} = -\frac{M_y}{M_x}, \tag{14}$$

and

$$\sigma = \frac{k\left(\boldsymbol{A}\cdot\delta\boldsymbol{B}\right)}{\delta B^2} = \frac{-2\cos\theta M_y\left(M_x - M_z\right)}{\cos^2\theta\left(M_x-M_z\right)^2 + M_y^2}, \tag{15}$$

where positive or negative helicity corresponds to the left-handed or the right-hand sense of rotation with respect to the wave vector $\boldsymbol{k}$, respectively. Here $\boldsymbol{A}$ is the vector potential, and the angular brackets denote an ensemble average over waves of random phase. The magnetic field and velocity perturbations are shown in Appendix B. For whistler waves, the dispersion relation and polarization properties of Equations (13) to (15) can be simplified in Appendix C.

To consider the validation of the charge-neutral condition, we define the ratio of electron to proton density perturbations

$$\frac{\delta n_e}{\delta n_i} = 1 + \left(\sin^2\theta\frac{M_x}{M} + \cos^2\theta\frac{M_z}{M}\right)\beta k^2\lambda_i^2\frac{v_A^2}{c^2}. \tag{16}$$

If $\delta n_\mathrm{e}/\delta n_\mathrm{i} = 1$, the number density of electrons equals to that of protons, while $\delta n_\mathrm{e}/\delta n_\mathrm{i} \neq 1$ implies that the charge-neutral condition is invalid. In the condition of $v_\mathrm{A}/c = 0$, $\delta n_\mathrm{e}/\delta n_\mathrm{i} = 1$ is satisfied for all modes.

We define the magnetic compressibility as (Gary & Smith 2009)

$$C_B = \frac{\delta B_z^2}{\delta B^2} = \frac{\sin^2\theta M_y^2}{M_y^2 + \cos^2\theta\left(M_x - M_z\right)^2}, \tag{17}$$

and the electron compressibility as (Podesta & TenBarge 2012)

$$\begin{aligned} C_\mathrm{e} &= \frac{\delta n_\mathrm{e}^2/n_0^2}{\delta B^2/B_0^2} \\ &= \frac{\omega^2/\omega_\mathrm{ci}^2\left[M + \left(\sin^2\theta M_\mathrm{x} + \cos^2\theta M_\mathrm{z}\right)\beta k^2\lambda_\mathrm{i}^2\frac{v_\mathrm{A}^2}{c^2}\right]^2}{\sin^2\theta k^4\lambda_\mathrm{i}^4\beta^2\left[M_\mathrm{y}^2 + \cos^2\theta\left(M_\mathrm{x} - M_\mathrm{z}\right)^2\right]}, \end{aligned} \tag{18}$$

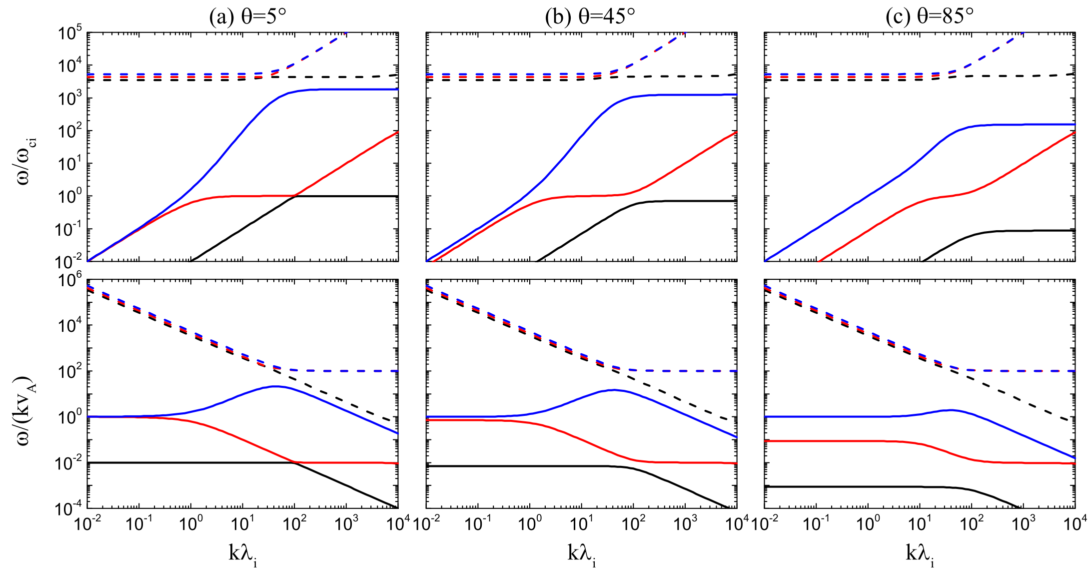

Fig. 1 Wave frequency and phase velocity as a function of the normalized wavenumber $k\lambda_{\rm i}$ at three propagation angles $\theta = 5°$, $45°$, and $85°$ in a low-beta plasma with $\beta = 10^{-4}$, $v_{\rm A}/c = 10^{-2}$, and $T_{\rm i}/T_{\rm e} = 1$, where the *black*, *red*, and *blue solid lines* correspond to the slow, Alfvén, and fast modes, and the *black*, *red*, and *blue dashed lines* represent the Langmuir, O, and X modes.

which describes the relationship between the electron number density and the perturbed magnetic field.

We also define the ratio of the electric field to magnetic field as follows (Wu 2012)

$$\frac{|\delta \boldsymbol{E}|}{|\delta \boldsymbol{B} v_{\rm A}|} = \frac{\omega/\omega_{\rm ci}\sqrt{\sin^2\theta M_{\rm x}^2 + \sin^2\theta M_{\rm y}^2 + \cos^2\theta M_{\rm z}^2}}{\sin\theta k\lambda_{\rm i}\sqrt{\cos^2\theta M_{\rm y}^2 + \cos^2\theta\left(M_{\rm x} - M_{\rm z}\right)^2 + \sin^2\theta M_{\rm y}^2}}. \tag{19}$$

3 DISPERSION RELATION AND POLARIZATION PROPERTIES

In the present section we analyze the dispersion relation and polarization properties of fast, Alfvén, and slow modes in the presence of a displacement current, and study the effects of the displacement current on the dispersion relation, polarization, helicity, and other properties. Based on the dispersion equation of Equation (13), Figure 1 presents the wave frequency $\omega/\omega_{\rm ci}$ and phase velocity $\omega/\left(kv_{\rm A}\right)$ versus the normalized wavenumber $k\lambda_{\rm i}$ in three different θ regimes: quasi-parallel propagation $\theta = 5°$, oblique propagation $\theta = 45°$ and quasi-perpendicular propagation $\theta = 85°$, where the black, red, and blue solid lines correspond to the slow, Alfvén, and fast modes, and the black, red, and blue dashed lines represent the Langmuir, O, and X modes. Other plasma parameters are $\beta = 10^{-4}$, $v_{\rm A}/c = 10^{-2}$, and $T_{\rm i}/T_{\rm e} = 1$.

From Figure 1, it is obvious that the general dispersion relation gives six roots for ω^2, which are divided into a low frequency group and a high frequency group. The low frequency group consists of the slow mode, Alfvén mode, and fast mode, and the high frequency group is shared by the Langmuir mode, O mode, and X mode (Boyd & Sanderson 2003). The slow mode corresponds to the slow magnetosonic wave at $\omega \ll \omega_{\rm ci}$ and the second ion cyclotron wave at $\omega \leq \omega_{\rm ci}\cos\theta$. The Alfvén mode becomes the shear Alfvén wave at $\omega \ll \omega_{\rm ci}$, the first ion cyclotron wave at $\omega \sim \omega_{ci}$, and the ion acoustic wave at $\omega_{\rm ci} < \omega < \omega_{\rm ce}\cos\theta$. The fast mode is the fast magnetosonic wave at $\omega \ll \omega_{\rm ci}$ and the whistler wave at $\omega_{\rm ci} < \omega < \omega_{\rm ce}\cos\theta$. It turns to the electron cyclotron wave at $\omega \sim \omega_{\rm ce}\cos\theta$. In addition, these modes have clearly separated phase velocities at all propagation angles except for $\theta = 0°$ and $90°$. It should be noted that only the low frequency group waves exist in the absence of the displacement current. In this paper, we focus on the low frequency group waves and the high frequency group waves have been neglected.

In the following, we discuss the effects of the displacement current on the wave dispersion relation and other properties. Using Equations (13) to (18), Figure 2 shows the wave frequency, phase velocity, and other properties versus the normalized wavenumber for the slow mode (black), Alfvén mode (red), and the fast mode (blue) at three different propagation angles $\theta = 5°$, $45°$, and $85°$, where the solid and dotted lines correspond to $v_{\rm A}/c = 0.1$ and 0, respectively. Here the plasma parameters $\beta =$

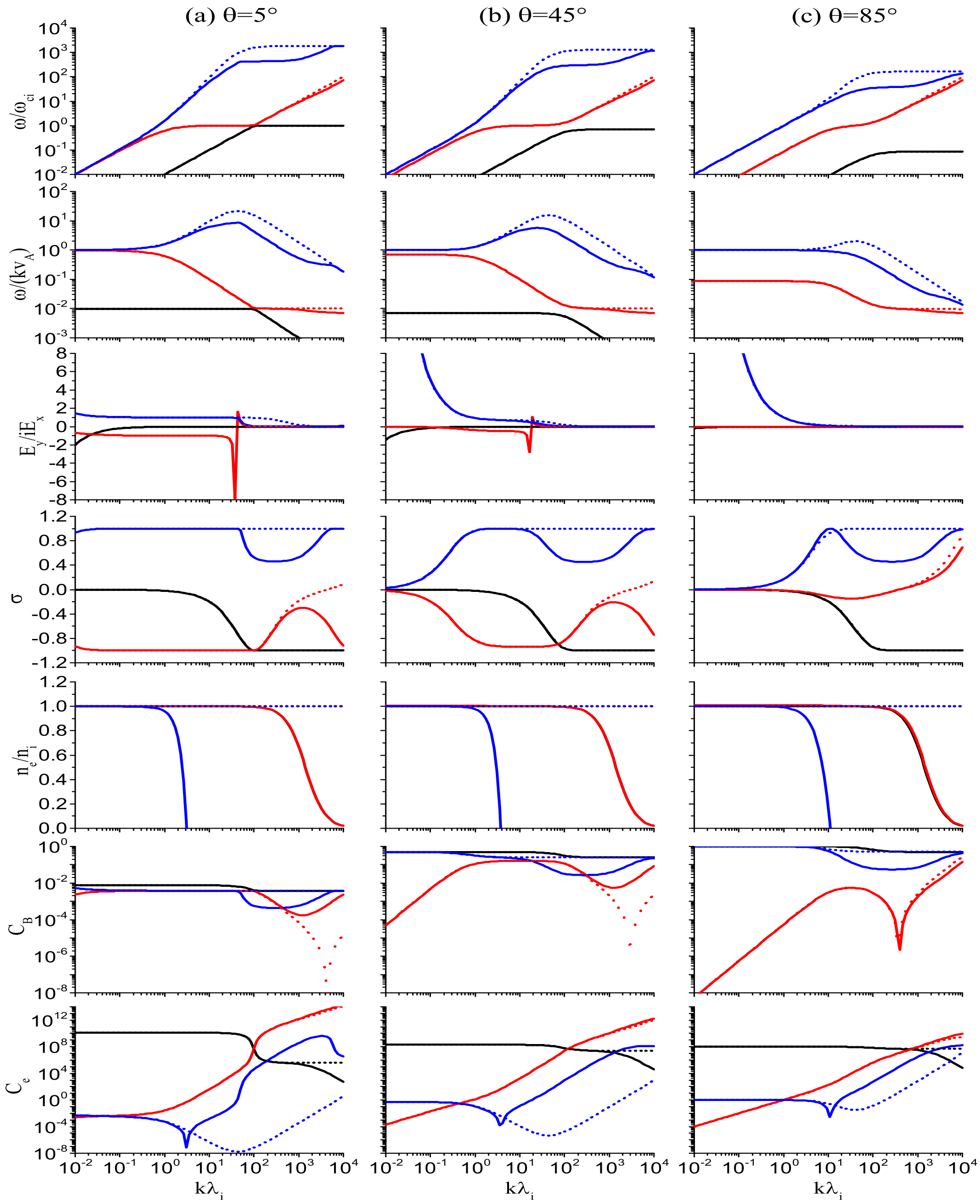

Fig. 2 Wave frequency and polarization properties of slow mode (*black*), Alfvén mode (*red*), and fast mode (*blue*) as a function of the normalized wavenumber $k\lambda_{\rm i}$ at three propagation angles $\theta = 5°$, $45°$, and $85°$ in a low-beta plasma with $\beta = 10^{-4}$ and $T_{\rm i}/T_{\rm e} = 1$, where the *solid* and *dotted lines* represent $v_{\rm A}/c = 0.1$ and 0, respectively.

10^{-4} and $T_{\rm i}/T_{\rm e} = 1$ have been used. As shown in Figure 2, the wave properties of both fast and Alfvén modes are sensitive to the displacement current, while the properties of the slow mode are weakly dependent on the displacement current. For both Alfvén and fast modes, the wave frequency and phase velocity with $\omega \geq \omega_{\rm ci}$ are smaller in the case of $v_{\rm A}/c = 0.1$ than that in the case of $v_{\rm A}/c = 0$, especially for the fast mode. At $\theta = 5°$ and $45°$, as $v_{\rm A}/c$ increases from 0 to 0.1, the magnetic helicity of the fast mode decreases from $\sigma = 1$ to $\simeq 0.5$, but that of Alfvén mode obviously decreases from $\sigma > 0$ to < 0, implying a helicity reversals of Alfvén mode from positive to negative value. It is also interesting to see that the charge-neutral conditions for both fast and Alfvén modes are invalid at $\omega \geq \omega_{\rm ci}$ (i.e., $n_{\rm e} \neq n_{\rm i}$), which correspond to different wavenumbers $k\lambda_{\rm i} \simeq 1$ and 100, respectively. Also, as $v_{\rm A}/c$ increases from 0 to 0.1, both the magnetic compressibility of the Alfvén mode and the electron compressibility of the fast mode increase. This indicates that the Alfvén mode has a relatively

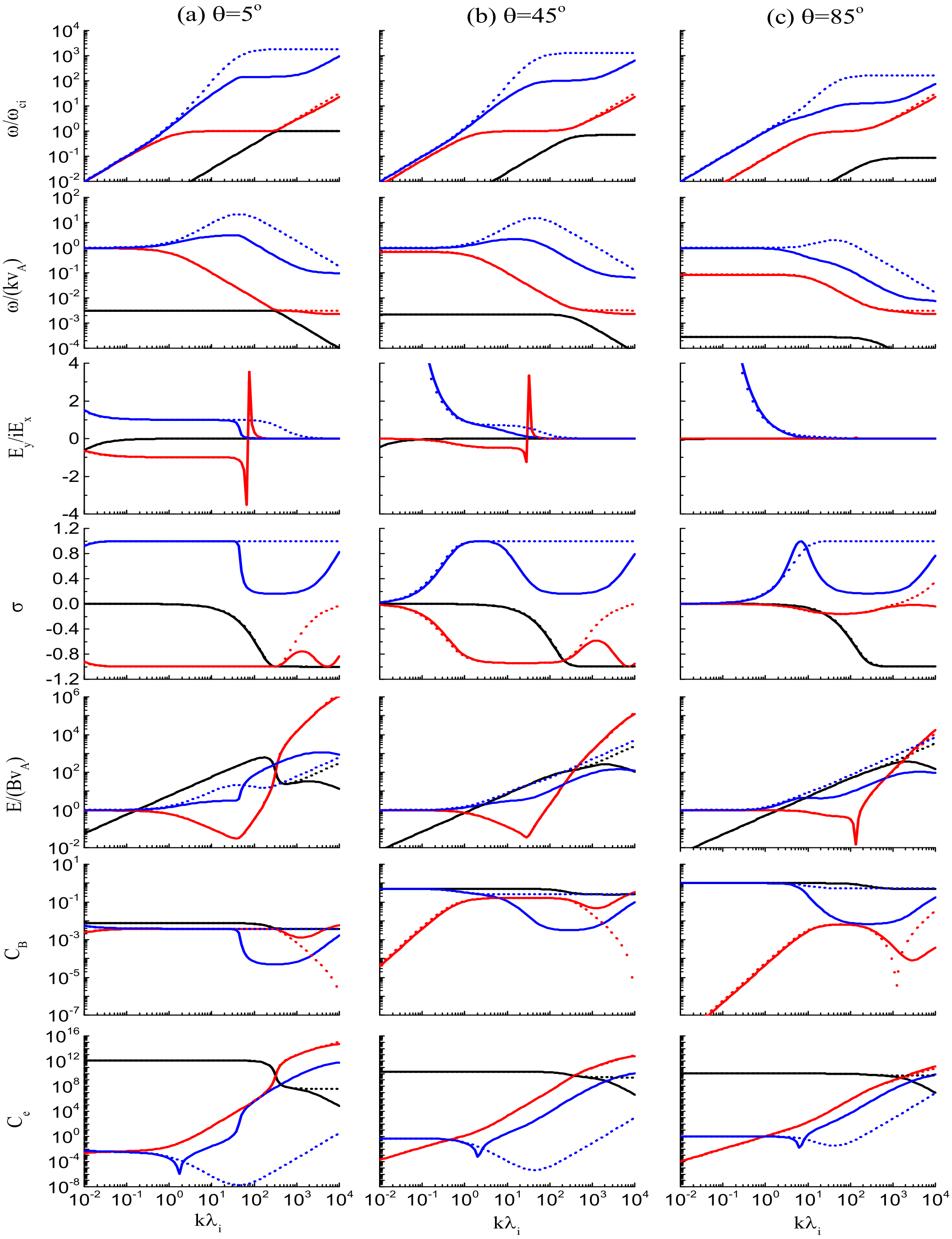

Fig. 3 Wave frequency and polarization properties of slow mode (*black*), Alfvén mode (*red*), and fast mode (*blue*) as a function of the normalized wavenumber $k\lambda_\mathrm{i}$ at three propagation angles $\theta = 5°$, $45°$, and $85°$ in a low-beta plasma with $\beta = 10^{-5}$ and $T_\mathrm{i}/T_\mathrm{e} = 1$, where the *solid* and *dotted lines* represent $v_\mathrm{A}/c = 0.3$ and 0, respectively.

large magnetic helicity and the fast mode becomes more compressible in the presence of the displacement current.

Figure 3 presents the dispersion relations, polarizations, and other properties for the slow mode (black), Alfvén mode (red), and fast mode (blue) at three propagation angles $\theta = 5°$, $45°$, and $85°$ in a low-beta plasma with $\beta = 10^{-5}$ and $T_\mathrm{i}/T_\mathrm{e} = 1$, where the solid and dotted lines correspond to $v_\mathrm{A}/c = 0.3$ and 0, respectively. Several mode properties in Figure 3 are obviously different from that in Figure 2. For example, for the fast mode at $k\lambda_\mathrm{i} \leq 10^3$, the wave frequency is $\omega/\omega_\mathrm{ci} < 200$ in $\beta = 10^{-5}$ and $v_\mathrm{A}/c = 0.3$ plasmas, but $\omega/\omega_\mathrm{ci} < 400$ in $\beta = 10^{-4}$ and $v_\mathrm{A}/c = 0.1$ plasmas. The fast mode has the magnetic helicity $\sigma \sim 0.2$ and the magnetic compressibility $C_\mathrm{B} \sim 10^{-5}$ in $\beta = 10^{-5}$ and $v_\mathrm{A}/c = 0.3$ plasmas. Moreover, the ratio of electric to magnetic fields

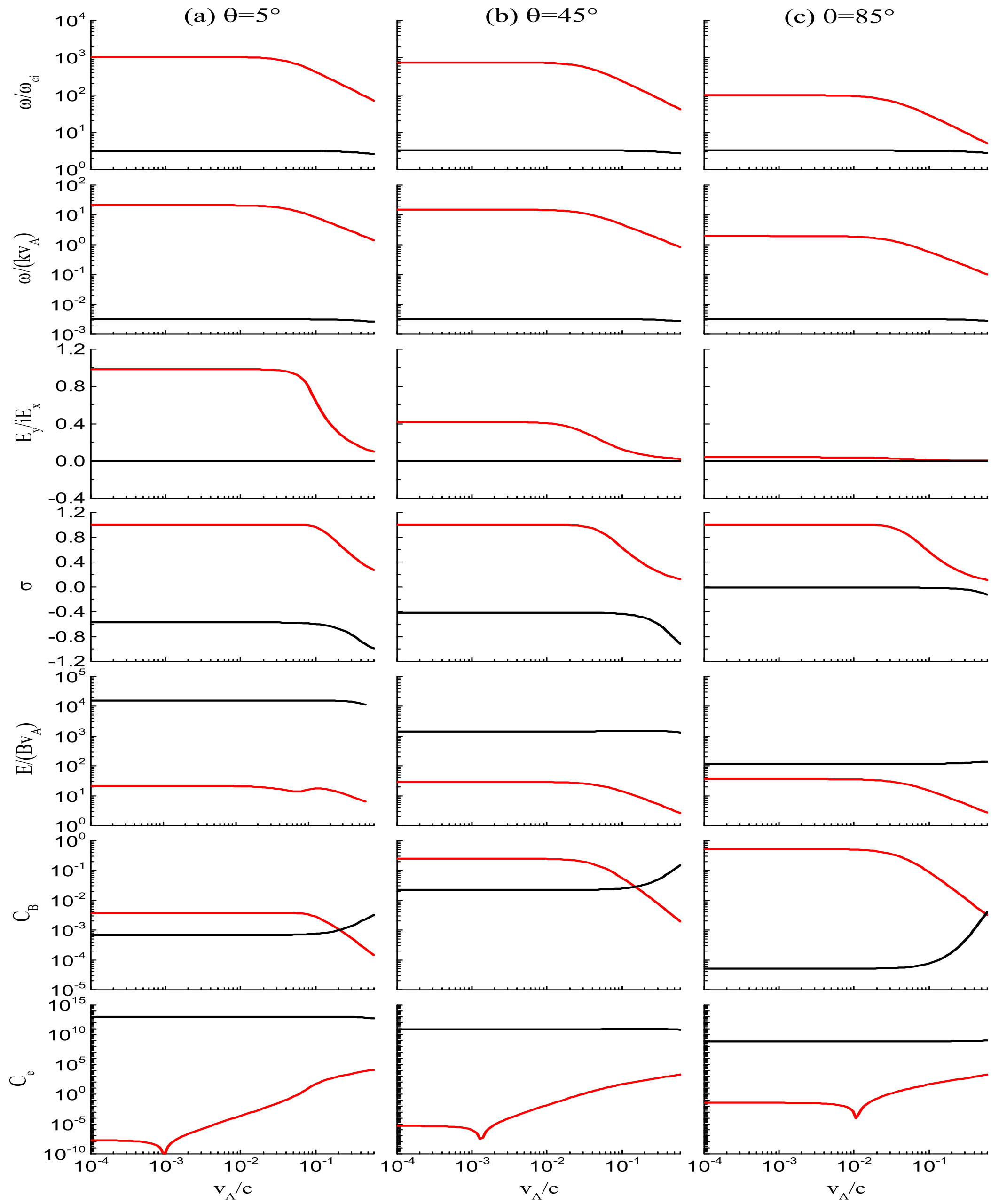

Fig. 4 Wave frequency and polarization properties versus the normalized Alfvén velocity $v_{\rm A}/c$ for the Alfvén mode at $k\lambda_{\rm i} = 10^3$ (*black*) and fast mode at $k\lambda_{\rm i} = 50$ (*red*) in a low-beta plasma with $\beta = 10^{-5}$, and $T_{\rm i}/T_{\rm e} = 1$, where panels (a), (b), and (c) correspond to different propagation angles $\theta = 5^\circ$, 45°, and 85°, respectively.

$E/(Bv_{\rm A})$ is affected by $v_{\rm A}/c$ for the fast mode, but not for the Alfvén mode.

Detailed variations of the dispersion relation and polarization properties with the normalized Alfvén velocity $v_{\rm A}/c$ are shown in Figure 4, where the black and red lines correspond to the Alfvén mode at $k\lambda_{\rm i} = 10^3$ and fast mode at $k\lambda_{\rm i} = 50$, respectively, and the plasma parameters are $\beta = 10^{-5}$, and $T_{\rm i}/T_{\rm e} = 1$. As shown in Figure 4, the wave frequency and other properties for both Alfvén and fast modes are sensitive to $v_{\rm A}/c$. In particular, both the wave frequency and phase velocity are nearly a constant for the Alfvén mode, but they vary significantly for the fast mode in the region of $10^{-2} < v_{\rm A}/c < 0.6$. The polarization $E_{\rm y}/iE_{\rm x}$ and the magnetic helicity σ for both modes are strongly affected by $v_{\rm A}/c$ when $v_{\rm A}/c > 0.1$, but not varied when $v_{\rm A}/c < 0.1$. For the fast mode, the ratio of electric to magnetic fields $E/(Bv_{\rm A})$ decreases with increasing $v_{\rm A}/c$ when $v_{\rm A}/c > 0.1$, while it is nearly a constant ($E/(Bv_{\rm A}) \sim 20$) when $v_{\rm A}/c < 0.1$. The magnetic compressibility increases with increasing

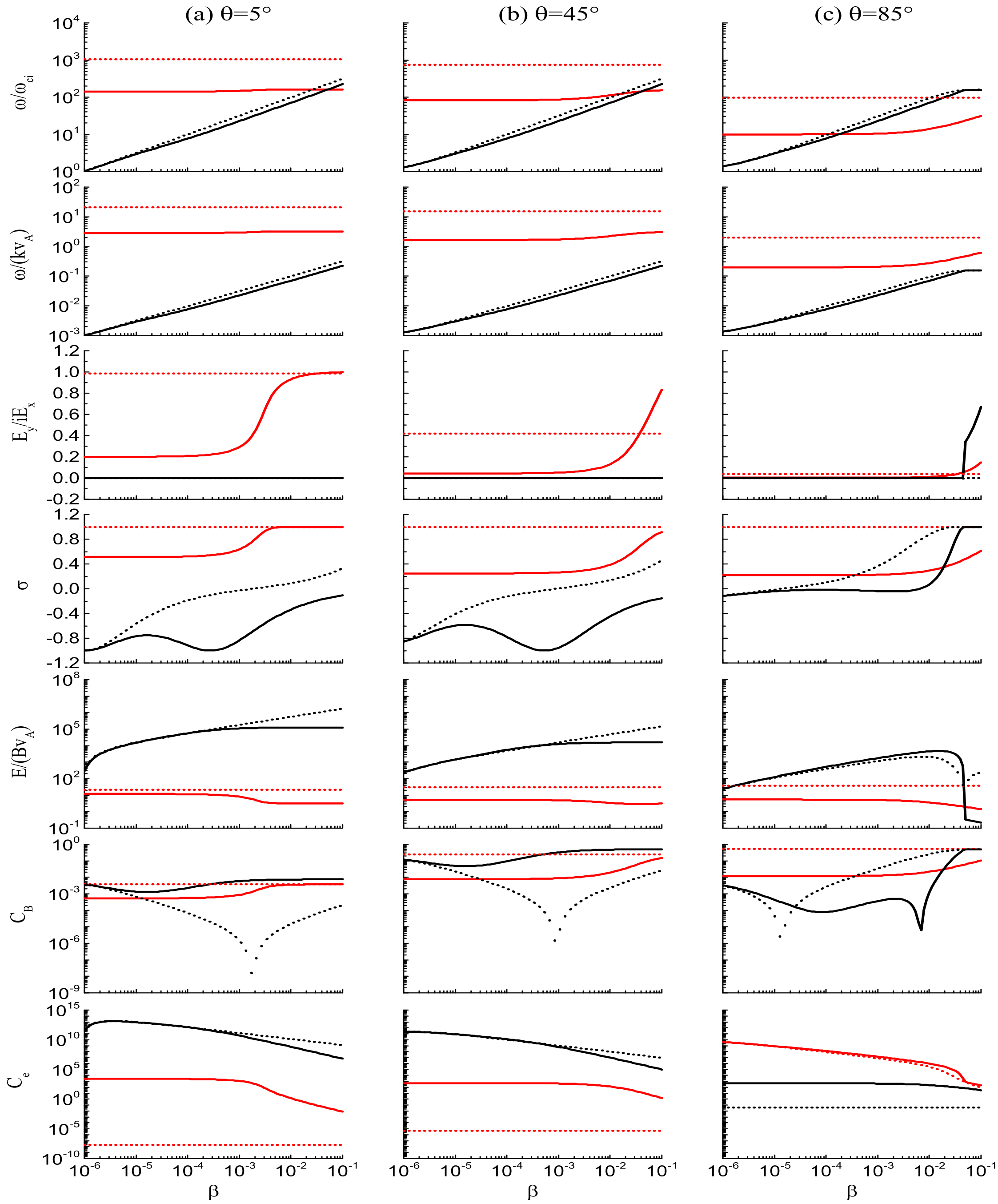

Fig. 5 Wave frequency and polarization properties versus the plasma beta β for the Alfvén mode at $k\lambda_{\rm i} = 10^3$ (*black*) and fast mode at $k\lambda_{\rm i} = 50$ (*red*) in a plasma with $T_{\rm i}/T_{\rm e} = 1$, where panels (a), (b), and (c) correspond to different propagation angles $\theta = 5°$, $45°$, and $85°$, respectively, and the *solid* and *dotted lines* in panels (a), (b), and (c) represent $v_{\rm A}/c = 0.3$ and 0, respectively.

$v_{\rm A}/c$ for the Alfvén mode, but it exhibits an opposite trend for the fast mode. Also, the electron compressibility significantly changes for the fast mode, while it is constant for the Alfvén mode.

Another important parameter in space and solar plasmas is the plasma beta β, which covers a wide range of $\beta < m_{\rm e}/m_{\rm i}$ in most auroral plasmas (Stasiewicz et al. 2000; Wu 2012). Figure 5 shows the dependence of the wave dispersion and other properties on the plasma beta β at $\theta = 5°$, $45°$, and $85°$ in a plasma with $v_{\rm A}/c = 0.3$ and $T_{\rm i}/T_{\rm e} = 1$, where the black and red lines represent the Alfvén mode at $k\lambda_{\rm i} = 10^3$ and fast mode at $k\lambda_{\rm i} = 50$, respectively, and the solid and dotted lines correspond to the cases of $v_{\rm A}/c = 0.3$ and 0. From

Figure 5, it can be found that the wave frequency and other properties sensitively depend on the plasma beta β. The fast mode has lower values of wave frequency, phase velocity, polarization, and magnetic helicity at $v_{\rm A}/c = 0.3$ than that at $v_{\rm A}/c = 0$ in the low-beta region of $\beta < 10^{-3}$, while the Alfvén mode presents the same results between $v_{\rm A}/c = 0$ and 0.3 in the high-beta region of $\beta > 10^{-2}$. For both the fast and Alfvén modes, the ratio of electric to magnetic fields $E/(Bv_{\rm A})$ decreases as $v_{\rm A}/c$ increases. Furthermore, as $v_{\rm A}/c$ increases from 0 to 0.3, the magnetic compressibility of the fast mode decreases at $\beta < 10^{-2}$, whereas that of the Alfvén mode increases at $\beta > 10^{-4}$. At $v_{\rm A}/c = 0$ the fast mode is incompressible, but it becomes more compressive at $v_{\rm A}/c = 0.3$, especially for the low-beta region of $\beta < 10^{-3}$. These results indicate the important role of the plasma beta β on both Alfvén and fast modes.

4 DISCUSSION AND CONCLUSION

In-situ measurements by the FREJA and FAST satellites have shown that plasma waves can be widely detected in the auroral plasma, including MHD Alfvén wave, kinetic Alfvén wave, ion-acoustic wave, ion cyclotron wave, fast wave, and whistler wave (Hofstee & Forsyth 1969; Cattell et al. 1998; Lund et al. 1998; Chaston et al. 2004, 2005; Wu & Chen 2020). These waves can efficiently transform the wave energy into the kinetic energy of plasma particles and can be responsible for the wave energy dissipation and particle energization in the auroral plasma (Lysak & Song 2003; Seyler & Liu 2007; Swift 2007; Wu 2012). In general, the polarization and helicity states of these waves could play an important role in the wave-particle interaction and have a potential importance in the physics of particle energization phenomena (Chen & Wu 2011). Moreover, the displacement current may be important in generating the parallel electric field, which can cause efficient heating or acceleration of plasma particles. However, there is still a lack of comprehensive investigations on the wave dispersion and polarization properties associating with the effects of a displacement current in auroral plasmas.

In the present paper, we investigate the wave dispersion relation and polarization properties in the presence of a displacement current in auroral plasmas, and the effects of the displacement current on these properties are also examined. Our results show that the displacement current can considerably affect the electromagnetic polarization properties for both fast and Alfvén modes, while the effect of the displacement current on the slow mode is minor. In particular, the fast mode with $\omega \geq \omega_{\rm ci}$ has relatively small wave frequency and relatively small phase velocity at $v_{\rm A}/c = 0.3$ as compared to that at $v_{\rm A}/c = 0$, but the variation for Alfvén and slow modes is insignificant. For fast and Alfvén modes, the magnetic helicity is obviously different with and without the displacement current, especially for the Alfvén mode with helicity reversals from $\sigma > 0$ to < 0 as $v_{\rm A}/c = 0$ to 0.3. Also, for fast and Alfvén modes, the charge-neutral condition is broken (i.e., $n_{\rm e}/n_{\rm i} \neq 1$) when $\omega \geq \omega_{\rm ci}$ in the condition of $v_{\rm A}/c = 0.3$, implying that the presence of the displacement current can lead to invalidation of the charge-neutral condition. The ratio of electric to magnetic fields $E/(Bv_{\rm A})$ is affected by $v_{\rm A}/c$ for the fast mode, but not for the Alfvén mode. Moreover, the Alfvén mode has relatively large magnetic compressibility and the fast mode has relatively large electron compressibility in the presence of the displacement current. In addition, the wave dispersion relation and polarization properties for both fast and Alfvén modes are different at different propagation angles θ, and sensitively depend on the plasma beta β and the normalized Alfvén velocity $v_{\rm A}/c$.

In-situ observations from the Juno spacecraft reported by Tetrick et al. (2017) have shown that a number of whistler activities exist in the high-latitude polar regions of Jupiters magnetosphere. The observed waves are located in the frequency range of $\sim$ 50 Hz – 40 kHz, and their frequencies are below the electron cyclotron frequency $\geq$ 40 kHz. The ratio of electric to magnetic fields is $E/cB \sim 0.5 - 3$. In our theoretical predications (see Fig. 3), the presence of $v_{\rm A}/c = 0.3$ can lead to lower frequency range of whistler waves with $\omega/\omega_{\rm ci} \leq 200$, which is consistent with the observed frequency distributions in Jupiter's high-latitude regions. Moreover, the theoretical prediction of the ratio of electric to magnetic fields for the whistler wave is $E/(cB) \sim 0.3 - 3$ (i.e., $E/(v_{\rm A}B) \sim 1 - 10$). This result can qualitatively explain the electromagnetic properties of the whistler wave in Jupiter's polar regions.

In summary, we revealed several new wave properties of fast and Alfvén modes accounting for the effects of a displacement current in auroral plasmas. These new properties can be of potential importance for a better understanding of wave modes and can be used in interpreting waves and turbulences at kinetic scales in auroral plasmas. It should be noted that the two-fluid theory cannot consider the kinetic wave-particle interaction effects, e.g., Landau damping and proton/electron cyclotron resonance damping. However, our results can be a useful guide to identify the wave modes in the kinetic theory and be conveniently used to compare with the results of the kinetic theory.

Acknowledgements This work was supported by the Science and Technology Innovation Program of Hunan Province (2020RC2049) and the National Natural Science Foundation of China under grants 12103018, 41531071, 11873018, 11690034, and 12075084. The authors thank Dr. J. S. Zhao for useful discussions and valuable suggestions. We give special thanks to the anonymous referee for the valuable suggestions and comments, which were helpful in improving the quality of this paper.

Appendix A: EXPRESSIONS OF M, M_X, M_Y, AND M_Z

The coefficients of M, M_x, M_y, and M_z in Equation (11) can be written as follows

$$\begin{aligned}
M=&\mathrm{a_3b_2c_1+a_3b_1c_2-a_2b_1c_3-a_1b_2c_3},\\
M_x=&\mathrm{b_2c_3d_1-b_1c_3d_2-\cot\theta b_2c_1d_3-\cot\theta b_1c_2d_3},\\
M_y=&\mathrm{a_3c_2d_1-a_2c_3d_1+a_3c_1d_2-a_1c_3d_2+\cot\theta a_2c_1d_3}\\
&-\cot\theta\mathrm{a_1c_2d_3},\\
M_z=&\tan\theta\mathrm{a_3b_2d_1}-\tan\theta\mathrm{a_3b_1d_2-a_2b_1d_3-a_1b_2d_3},
\end{aligned} \quad (A.1)$$

with the plasma parameters

$$\begin{aligned}
a_1=&\cos^2\theta\Lambda_0\Lambda_2\left(1-\frac{1}{\cos^2\theta}\frac{v_A^2}{c^2}\frac{1}{k^2\lambda_i^2}\frac{\omega^2}{\omega_{ci}^2}\right)k^2\lambda_i^2\\
&-\left[(1+Q)\Lambda_1+\sin^2\theta Q\Lambda_0\frac{v_A^2}{c^2}k^2\lambda_i^2\beta\tilde{T}_e\right]\frac{\omega^2}{\omega_{ci}^2},\\
b_1=&\left(1-Q^2\right)\frac{\omega^3}{\omega_{ci}^3},\\
c_1=&\sin\theta\cos\theta\Lambda_0\left(\Lambda_2+Q\frac{v_A^2}{c^2}\beta\frac{\omega^2}{\omega_{ci}^2}\tilde{T}_e\right)k^2\lambda_i^2,\\
d_1=&\left(\Lambda_2\tilde{T}_i-Q\Lambda_0\tilde{T}_e\right)\frac{\omega^2}{\omega_{ci}^2},\\
a_2=&\left(1-Q^2\right)\frac{\omega^3}{\omega_{ci}^3}-\sin^2\theta\Lambda_0\frac{v_A^2}{c^2}\beta k^2\lambda_i^2\frac{\omega}{\omega_{ci}}\tilde{T}_e,\\
b_2=&(1+Q)\Lambda_1\frac{\omega^2}{\omega_{ci}^2}-\Lambda_0\Lambda_2\left(1-\frac{v_A^2}{c^2}\frac{1}{k^2\lambda_i^2}\frac{\omega^2}{\omega_{ci}^2}\right)k^2\lambda_i^2,\\
c_2=&\sin\theta\cos\theta\Lambda_0\frac{v_A^2}{c^2}\beta k^2\lambda_i^2\frac{\omega}{\omega_{ci}}\tilde{T}_e,\\
d_2=&\left(\Lambda_2\tilde{T}_i+\Lambda_0\tilde{T}_e\right)\frac{\omega}{\omega_{ci}},\\
a_3=&\sin\theta\cos\theta\left(Q-\frac{v_A^2}{c^2}\beta\tilde{T}_e\right)k^2\lambda_i^2,\\
c_3=&1+Q+\sin^2\theta Qk^2\lambda_i^2\left(1-\frac{1}{\sin^2\theta}\frac{1}{k^2\lambda_i^2}\frac{v_A^2}{c^2}\frac{\omega^2}{\omega_{ci}^2}\right)\\
&+\cos^2\theta\frac{v_A^2}{c^2}\beta\tilde{T}_ek^2\lambda_i^2,\\
d_3=&\left(Q\tilde{T}_i-\tilde{T}_e\right),
\end{aligned} \quad (A.2)$$

where

$$\Lambda_1=1-Q\omega^2/\omega_{ci}^2. \quad (A.3)$$

Appendix B: MAGNETIC FIELD AND VELOCITY PERTURBATIONS

From Equations (1) to (6), the magnetic field and velocity perturbations can be expressed in terms of the number density perturbation of ions as follows:

$$\begin{aligned}
\frac{\delta B_x}{B_0}&=-\sin\theta\cos\theta\frac{1}{\omega/\omega_{ci}}k^2\lambda_i^2\beta\frac{M_y}{M}\frac{\delta n_i}{n_0},\\
\frac{\delta B_y}{B_0}&=i\sin\theta\cos\theta\frac{1}{\omega/\omega_{ci}}k^2\lambda_i^2\beta\frac{M_x-M_z}{M}\frac{\delta n_i}{n_0},\\
\frac{\delta B_z}{B_0}&=\sin^2\theta\frac{1}{\omega/\omega_{ci}}k^2\lambda_i^2\beta\frac{M_y}{M}\frac{\delta n_i}{n_0},
\end{aligned} \quad (B.1)$$

$$\begin{aligned}
\frac{\delta v_{ix}}{v_T}&=\sin\theta\frac{1}{\Lambda_0}\left(\frac{M_y}{M}+\frac{M_x}{M}\frac{\omega}{\omega_{ci}}-\tilde{T}_i\frac{\omega}{\omega_{ci}}\right)\sqrt{\beta}k\lambda_i\frac{\delta n_i}{n_0},\\
\frac{\delta v_{iy}}{v_T}&=i\sin\theta\frac{1}{\Lambda_0}\left(-\frac{M_x}{M}-\frac{M_y}{M}\frac{\omega}{\omega_{ci}}+\tilde{T}_i\right)\sqrt{\beta}k\lambda_i\frac{\delta n_i}{n_0},\\
\frac{\delta v_{iz}}{v_T}&=\cos\theta\frac{1}{\omega/\omega_{ci}}\left(-\frac{M_z}{M}+\tilde{T}_i\right)\sqrt{\beta}k\lambda_i\frac{\delta n_i}{n_0},
\end{aligned} \quad (B.2)$$

and

$$\begin{aligned}
\frac{\delta v_{ex}}{v_T}=&\sin\theta\frac{1}{\Lambda_2}\sqrt{\beta}k\lambda_i\frac{\delta n_i}{n_0}\left(\frac{M_y}{M}-Q\frac{\omega}{\omega_{ci}}\frac{M_x}{M}\right)\\
&-\sin\theta\frac{1}{\Lambda_2}\sqrt{\beta}k\lambda_i\frac{\delta n_i}{n_0}Q\frac{\omega}{\omega_{ci}}\tilde{T}_e\\
&\times\left[1+\left(\sin^2\theta\frac{M_x}{M}+\cos^2\theta\frac{M_z}{M}\right)\beta k^2\lambda_i^2\frac{v_A^2}{c^2}\right],\\
\frac{\delta v_{ey}}{v_T}=&i\sin\theta\frac{1}{\Lambda_2}\sqrt{\beta}k\lambda_i\frac{\delta n_i}{n_0}\left(-\frac{M_x}{M}+Q\frac{\omega}{\omega_{ci}}\frac{M_y}{M}\right)\\
&-i\sin\theta\frac{1}{\Lambda_2}\sqrt{\beta}k\lambda_i\frac{\delta n_i}{n_0}\tilde{T}_e\\
&\times\left[1+\left(\sin^2\theta\frac{M_x}{M}+\cos^2\theta\frac{M_z}{M}\right)\beta k^2\lambda_i^2\frac{v_A^2}{c^2}\right]\tilde{T}_e,\\
\frac{\delta v_{ez}}{v_T}=&\cos\theta\frac{1}{Q}\frac{1}{\omega/\omega_{ci}}\sqrt{\beta}k\lambda_i\frac{\delta n_i}{n_0}\\
&\times\left\{\frac{M_z}{M}+\tilde{T}_e\left[1+\left(\sin^2\theta\frac{M_x}{M}+\cos^2\theta\frac{M_z}{M}\right)\beta k^2\lambda_i^2\frac{v_A^2}{c^2}\right]\right\}.
\end{aligned} \quad (B.3)$$

Appendix C: DISPERSION RELATION AND POLARIZATION PROPERTIES OF WHISTLER WAVES

For the whistler waves, at the frequency condition of $\omega \ll \min[\omega_{ce},\omega_{pe},ck]$, the dispersion relation in Equation (13) can be simplified as follows (Zhao 2017)

$$\frac{\omega}{\omega_{ci}}=\frac{\cos\theta k^2\lambda_i^2}{1+Qk^2\lambda_i^2}\sqrt{\frac{1+\frac{T_e}{T_i}k^2\lambda_i^2\frac{v_{Ti}^2}{v_A^2}\frac{v_A^2}{c^2}}{1+\frac{T_e}{T_i}k^2\lambda_i^2\frac{v_{Ti}^2}{v_A^2}\frac{v_A^2}{c^2}+\frac{k^2\lambda_i^2}{1+Qk^2\lambda_i^2}\frac{v_A^2}{c^2}}}, \quad (C.1)$$

which describes the dispersion relation of the whistler wave including the effects of v_A/c.

For the frequency limit of $\omega \ll \min[\omega_{\rm ce}, \omega_{\rm pe}, ck]$, the polarization and the magnetic helicity in Equations (14) and (15) can be reduced to

$$\frac{E_{\rm y}}{iE_{\rm x}} = -\frac{\frac{\omega^2}{\omega_{\rm ci}^2}\left(1+Qk^2\lambda_{\rm i}^2\right)^2 - \cos^2\theta k^4\lambda_{\rm i}^4}{\frac{\omega^3}{\omega_{\rm ci}^3}\left(1+Qk^2\lambda_{\rm i}^2\right)\frac{v_{\rm A}^2}{c^2}} + \frac{\cos^2\theta k^2\lambda_{\rm i}^2}{\frac{\omega}{\omega_{\rm ci}}\left(1+Qk^2\lambda_{\rm i}^2\right)}, \tag{C.2}$$

and

$$\sigma = \frac{2\cos^2\theta A\left(\cos\theta - i\sin\theta B\right)}{\cos^2\theta\left(\cos\theta - i\sin\theta B\right)^2 - \cos^2\theta A^2}, \tag{C.3}$$

where

$$A = -\frac{\frac{\omega^2}{\omega_{\rm ci}^2}\left(1+Qk^2\lambda_{\rm i}^2\right)^2 - \cos^2\theta k^4\lambda_{\rm i}^4}{\frac{\omega^3}{\omega_{\rm ci}^3}\left(1+Qk^2\lambda_{\rm i}^2\right)\frac{v_{\rm A}^2}{c^2}} + \frac{\cos^2\theta k^2\lambda_{\rm i}^2}{\frac{\omega}{\omega_{\rm ci}}\left(1+Qk^2\lambda_{\rm i}^2\right)}, \tag{C.4}$$

and

$$B = -\frac{\cos\theta}{\sin\theta}\frac{\frac{\omega^2}{\omega_{\rm ci}^2}\left(1+Qk^2\lambda_{\rm i}^2\right)^2 - \cos^2\theta k^4\lambda_{\rm i}^4}{\frac{\omega^3}{\omega_{\rm ci}^3}\left(1+Qk^2\lambda_{\rm i}^2\right)\frac{v_{\rm A}^2}{c^2}} + \sin\theta\cos\theta\frac{k^2\lambda_{\rm i}^2}{\frac{\omega}{\omega_{\rm ci}}\left(1+Qk^2\lambda_{\rm i}^2\right)}. \tag{C.5}$$

From Equations (C.2) and (C.3), it is clear that the polarization and the magnetic helicity obtained by Zhao (2017) may be recovered by setting $\omega \ll \min[\omega_{\rm ce}, \omega_{\rm pe}, ck]$.

References

Andre, M. 1985, Journal of Plasma Physics, 33, 1

Bellan, P. M. 2012, Journal of Geophysical Research (Space Physics), 117, A12219

Bespalov, P. A., Misonova, V. G., & Cowley, S. W. H. 2006, Annales Geophysicae, 24, 2313

Boldyrev, S., Horaites, K., Xia, Q., & Perez, J. C. 2013, ApJ, 777, 41

Boyd, T. J. M., & Sanderson, J. J. 2003, The Physics of Plasmas (Cambridge, UK: Cambridge Univ. Press)

Cattell, C., Bergmann, R., Sigsbee, K., et al. 1998, Geophys. Res. Lett., 25, 2053

Chaston, C. C., Bonnell, J. W., Carlson, C. W., et al. 2004, Journal of Geophysical Research (Space Physics), 109, A04205

Chaston, C. C., Peticolas, L. M., Carlson, C. W., et al. 2005, Journal of Geophysical Research (Space Physics), 110, A02211

Chen, L., & Wu, D. J. 2011, Physics of Plasmas, 18, 072110

Cramer, N. F. 2001, The Physics of Alfvén Waves (Wiley-VCH)

Gary, S. P. 1986, Journal of Plasma Physics, 35, 431

Gary, S. P., & Borovsky, J. E. 2004, Journal of Geophysical Research (Space Physics), 109, A06105

Gary, S. P., & Smith, C. W. 2009, Journal of Geophysical Research (Space Physics), 114, A12105

Hofstee, J., & Forsyth, P. A. 1969, Canadian Journal of Physics, 47, 2797

Hollweg, J. V. 1999, J. Geophys. Res., 104, 14811

Kaufmann, R. L. 1984, Space Sci. Rev., 37, 313

Kletzing, C. A., Mozer, F. S., & Torbert, R. B. 1998, J. Geophys. Res., 103, 14837

Kletzing, C. A., & Torbert, R. B. 1994, J. Geophys. Res., 99, 2159

Lu, Q., & Li, X. 2007, Physics of Plasmas, 14, 042303

Lund, E. J., Möbius, E., Tang, L., et al. 1998, Geophys. Res. Lett., 25, 2049

Lysak, R. L., & Lotko, W. 1996, J. Geophys. Res., 101, 5085

Lysak, R. L., & Song, Y. 2003, Journal of Geophysical Research (Space Physics), 108, 8005

Mozer, F. S., Cattell, C. A., Hudson, M. K., et al. 1980, Space Sci. Rev., 27, 155

Podesta, J. J., & TenBarge, J. M. 2012, Journal of Geophysical Research (Space Physics), 117, A10106

Sahraoui, F., Belmont, G., & Goldstein, M. L. 2012, ApJ, 748, 100

Seyler, C. E., & Liu, K. 2007, Journal of Geophysical Research (Space Physics), 112, A09302

Stasiewicz, K., Bellan, P., Chaston, C., et al. 2000, Space Sci. Rev., 92, 423

Swanson, D. G. 2003, Plasma Waves, 2nd Edition (Taylor & Francis)

Swift, D. W. 2007, Journal of Geophysical Research (Space Physics), 112, A12207

Tetrick, S. S., Gurnett, D. A., Kurth, W. S., et al. 2017, Geophys. Res. Lett., 44, 4447

Wu, D. J., & Chao, J. K. 2003, Physics of Plasmas, 10, 3787

Wu, D. J., & Chao, J. K. 2004, Journal of Geophysical Research (Space Physics), 109, A06211

Wu, D. J. 2012, Kinetic Alfvén Waves: Theory, Experience, and Application (Beijing: Science Press)

Wu, D. J. & Chen, L. 2020, Kinetic Alfvén Waves in Laboratory, Space, and Astrophysical Plasmas (Nanjing: Nanjing Univ. Press)

Xiang, L., Chen, L., & Wu, D. J. 2019, ApJ, 881, 61

Zhao, J. 2015, Physics of Plasmas, 22, 042115

Zhao, J. 2017, ApJ, 850, 13

Zhao, J. S., Voitenko, Y., Yu, M. Y., Lu, J. Y., & Wu, D. J. 2014, ApJ, 793, 107